Diurnal cycle of summertime deep convection over North America: A satellite perspective

Baijun Tian[1]
Atmospheric and Oceanic Sciences Program, Princeton University, Princeton, New Jersey, USA

Isaac M. Held, Ngar-Cheung Lau, and Brian J. Soden
Geophysical Fluid Dynamics Laboratory, NOAA, Princeton, New Jersey, USA

Received 23 July 2004; revised 22 December 2004; accepted 21 January 2005; published 26 April 2005.

[1] High-resolution ($0.1^\circ \times 0.1^\circ$) geostationary satellite infrared radiances at 11 μm in combination with gridded ($2.5^\circ \times 2.0^\circ$) hourly surface precipitation observations are employed to document the spatial structure of the diurnal cycle of summertime deep convection and associated precipitation over North America. Comparison of the diurnal cycle pattern between the satellite retrieval and surface observations demonstrates the reliability of satellite radiances for inferring the diurnal cycle of precipitation, especially the diurnal phase. On the basis of the satellite radiances, we find that over most land regions, deep convection peaks in the late afternoon and early evening, a few hours later than the peak of land surface temperature. However, strong regional variations exist in both the diurnal phase and amplitude, implying that topography, land-sea contrast, and coastline curvature play an important role in modulating the diurnal cycle. Examples of such effects are highlighted over Florida, the Great Plains, and the North American monsoon region.

Citation: Tian, B., I. M. Held, N.-C. Lau, and B. J. Soden (2005), Diurnal cycle of summertime deep convection over North America: A satellite perspective, *J. Geophys. Res.*, *110*, D08108, doi:10.1029/2004JD005275.

1. Introduction

[2] The diurnal cycle of tropical deep convection and associated precipitation is of intrinsic interest with studies dating back several decades [e.g., *Wallace*, 1975; *Gray and Jacobson*, 1977; *Yang and Slingo*, 2001]. The studies using global data sets indicate that there is a clear land-sea contrast in the diurnal cycle of tropical convection [e.g., *Yang and Slingo*, 2001; *Tian et al.*, 2004]. Over land, the diurnal variation is strong, and maximum convection occurs in the late afternoon and early evening. In contrast, it is relatively weak over the oceans with peaks in the morning. While the physical mechanisms behind the oceanic diurnal cycle are still unclear, the diurnal cycle of continental convection can be mainly attributed to a direct thermodynamic response to the strong diurnal cycle of solar heating land surface temperature, and atmospheric stability [*Wallace*, 1975; *Yang and Slingo*, 2001; *Tian et al.*, 2004].

[3] However, strong regional variations in diurnal cycle are found over many inland and coastal regions of the world, highlighting the importance of land-sea breezes and mountain-valley winds as well as coastline curvature in modulating the diurnal cycle [e.g., *Yang and Slingo*, 2001; *Ohsawa et al.*, 2001; *Mapes et al.*, 2003a, 2003b; *Zuidema*, 2003]. For example, *Yang and Slingo* [2001] suggested that the diurnal phase and amplitude over Africa and South America is in part modulated by the local orography. They also noted that the strong diurnal signal over land is spread out over the adjacent oceans, such as the Bay of Bengal, probably through gravity waves of varying depths. Through investigating the physical processes related to the rainfall climate over the Panama Bight and Pacific littoral of Colombia, *Mapes et al.* [2003a, 2003b] described how the mesoscale structure of the diurnal cycle in that region is controlled by the complex coastlines and topography.

[4] Complex topography and coastlines are also found over North America (NA) (Figure 1), such as the orography contrast between the Rocky Mountains and the Great Plains, and coastline curvature around the Florida peninsula. In northwestern Mexico, the core NA monsoon (NAM) region, the mountains of the Sierra Madre Occidental (SMO) are located near the coast, next to the Gulf of California (GC), resulting in both strong mountain-valley and land-sea contrasts in this region. Thus detailed mesoscale structures in the diurnal cycle over NA are expected. As a result, high-spatial-resolution and high-temporal-resolution data that are able to resolve the land-sea contrast, coastline curvature, mountains and valleys are required to study the diurnal cycle over NA.

[5] Most previous studies on the diurnal cycle over NA have relied on a gridded, 2.5° longitude by 2.0° latitude, hourly precipitation data set produced by *Higgins et al.* [1996] from quality-controlled station records over the

[1]Now at Division of Geological and Planetary Sciences, California Institute of Technology, Pasadena, California, USA.

0148-0227/05/2004JD005275$09.00

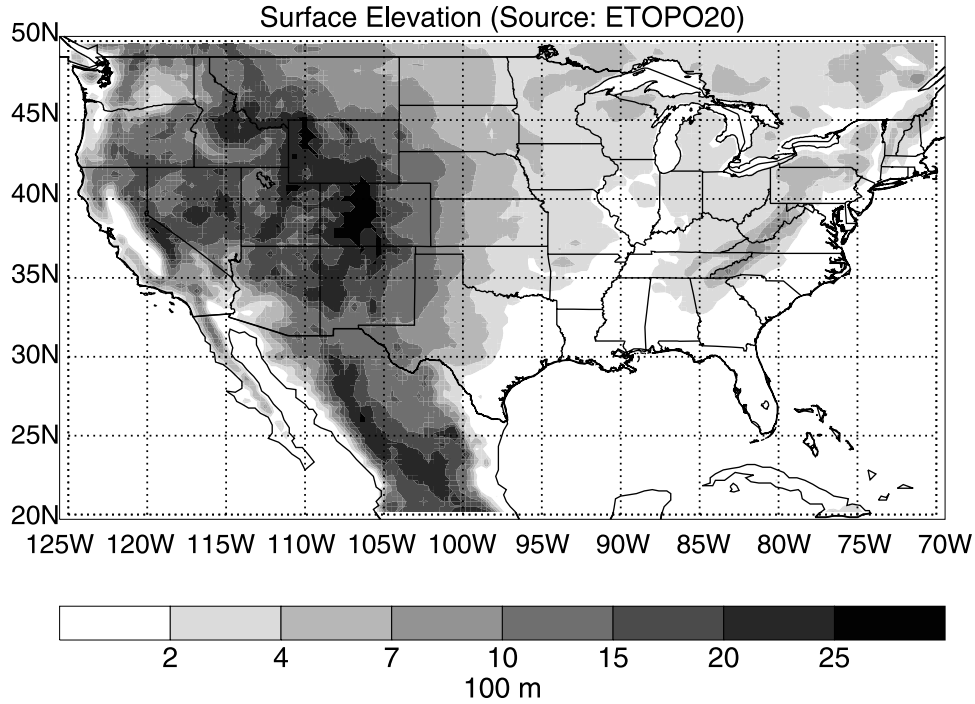

Figure 1. Surface elevation over North America (NA) based on 20-min topographic data. See color version of this figure in the HTML.

United States [e.g., *Higgins et al.*, 1997; *Dai et al.*, 1999]. Other studies relied directly on surface station records over limited regions of the US [e.g., *Wallace*, 1975; *Schwartz and Bosart*, 1979; *Riley et al.*, 1987; *Landin and Bosart*, 1989]. In particular, because of the sparse quality surface station data over Mexico, the diurnal cycle of the NAM precipitation is poorly documented. *Negri et al.* [1993, 1994] presented the warm season rainfall for the southwest United States and Mexico derived from high-spatial-resolution Special Sensor Microwave Imager (SSM/I) and examined the diurnal cycle. However, because of the limitation of the polar-orbiting satellites, the morning and evening overpass times cannot fully resolve the diurnal cycle in these studies. In summary, due mainly to the lack of high spatial and temporal resolution surface or satellite data, the spatial structure of the diurnal cycle over NA has not been fully explored by the previous studies. This is particularly true over the NAM region, even though most of the rainfall in this region is diurnal [*U.S. CLIVAR Pan American Implementation Panel*, 2002] (see also http://www.cpc.ncep.noaa.gov/products/precip/monsoon/NAME.html). The IR radiances at the 11 μm channel from geostationary satellites offer unmatched spatial and temporal resolutions and have been widely applied to study the diurnal cycle of tropical deep convection and precipitation [e.g., *Meisner and Arkin*, 1987; *Yang and Slingo*, 2001; *Mapes et al.*, 2003a; *Tian et al.*, 2004], making them an ideal data source for studying the spatial structure of the diurnal cycle over NA.

[6] Furthermore, it is very common for the global and regional climate models do poorly in simulating the diurnal cycle, such as the National Center for Atmospheric Research Community Climate System Model [*Trenberth et al.*, 2003], the Geophysical Fluid Dynamics Laboratory AM2 [*Tian et al.*, 2004], and the Met Office United Model [*Yang and Slingo*, 2001]. Since radiation budget and latent heat flux are strongly linked to the timing of deep convection, the poor simulation of the diurnal cycle of convection in models may be an important contributor to the systematic biases in mean climate. For example, experiments with a climate version of the Met Office model (HadAM3) by *Neale and Slingo* [2003] show that the HadAM3 has substantial errors in its simulation of the diurnal cycle over the islands of the maritime continent, which can rectify onto the seasonal mean climate. Furthermore, they argued that deficient rainfall over the Maritime Continent could be a driver for other systematic errors in the model, such as the excess precipitation over the western Indian Ocean. Thus improving the diurnal cycle simulation in climate models may be the key for improving the mean climate simulation. Naturally, we hope that the diurnal cycle analysis based on high-spatial-resolution and high-temporal-resolution satellite radiances as we performed here will be useful to the climate modelers to improve the diurnal cycle simulation in climate models.

[7] The purposes of this study are twofold: First, we assess the reliability of satellite radiances for inferring the diurnal cycle of precipitation by comparing satellite retrievals with surface precipitation observations, which are both available over the United States for the year 1999. Second, relying on the high-resolution ($0.1^\circ \times 0.1^\circ$, every 3 hours) satellite radiances, we document the spatial structure of the diurnal cycle of summertime deep convection and precipitation over NA. The outline for the rest of this paper is as follows: The satellite radiances, method of precipitation retrieval from radiances, surface precipitation observations, and diurnal cycle analysis method are described in section 2. Section 3 will present a comparison of the diurnal cycles

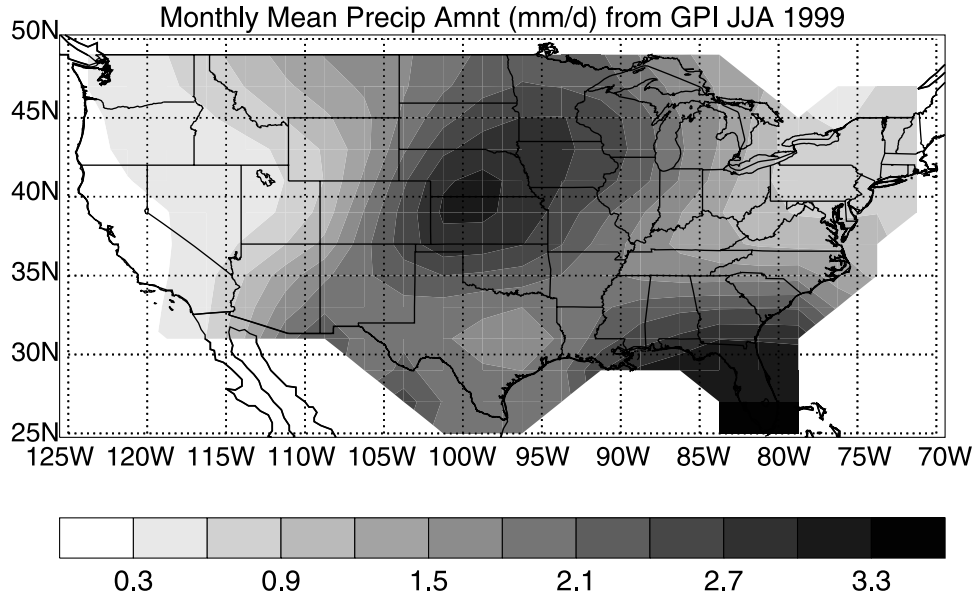

Figure 2. Summertime mean precipitation over the United States with resolution 2.5° longitude by 2.0° latitude based on satellite data (GOES precipitation index) for 1999. See color version of this figure in the HTML.

between satellite retrievals and surface observations over the United States. The diurnal cycle of summertime deep convection over NA for 1999 based on the high-resolution satellite radiances is discussed in section 4. Conclusions are summarized in section 5.

2. Data and Method

[8] The primary data for this study are geostationary satellite IR radiances (expressed as equivalent blackbody temperatures) in the window (11 μm) channel (T_{11}) from GOES 10 (180°–105°W) and GOES 8 (105°W–35°W). The data cover the year 1999 at a temporal resolution of 3 hours and a spatial resolution of 0.1° × 0.1° longitude-latitude. Details regarding radiance measurements and satellite intercalibration are given by *Tian et al.* [2004]. The independent surface precipitation observations for this study are from the updated *Higgins et al.* [1996], a gridded hourly precipitation data set constructed from quality-controlled surface station records over the United States using a spatial and temporal interpolation. The data cover the period from 1943 to 2002 and have a spatial resolution of 2.5° longitude by 2.0° latitude.

[9] To retrieve precipitation from the satellite radiances, we rely on the simplest GOES precipitation index (GPI) originally developed by *Arkin and Meisner* [1987] as follows,

$$\mathrm{GPI} = aF_c \tag{1}$$

F_c is the fractional coverage of deep convective clouds ($T_{11} < 230$ K) within a large-scale grid box (2.5° longitude by 2.0° latitude) or a high-resolution pixel (0.1° × 0.1° longitude-latitude). In the latter case, F_c equals either 100% or 0, and a long time average is required, such as a season in our case, in order for the GPI to be meaningful. Here a is a constant factor 3 mm h^{-1} within the tropics (25°S–25°N) and linearly decreases poleward because of the zenith angle dependence of the satellite radiances [*Joyce and Arkin*, 1997].

[10] Comparing the precipitation between satellite retrieval (Figure 2) and surface observations (Figure 3) indicates that the satellite retrieval is comparable to the surface observations in magnitude and spatial pattern. Both data sets show that strong precipitation is found over Florida and the Midwest, while dry conditions are common over western and northeastern United States. However, significant difference is found over the Great Plains, where the satellite retrieval is twice as large as surface observation. This difference may be due to the deficiency of the simplest GPI algorithm and/or different sampling locations for satellite and surface observations. For example, the condensation associated with the deep convective clouds over this region may be reevaporated before falling to the ground, causing the deep convective cloud index to exceed the observed rainfall at the surface. A similar difference between microwave retrieval and surface observations is also found for the United States (E. Wilcox, personal communication, 2004). This systematic bias in the mean will result in systematic bias in diurnal magnitude over the Great Plains but should not be a serious problem for diurnal phase.

[11] It is worth noting that our usage of GPI in this study has pushed the GPI beyond its realm of calibrated validity by calculating precipitation at high-resolution (0.1° × 0.1°), in midlatitudes, and at different times of day. Because of this concern, *Garreaud and Wallace* [1997] omitted the 3 mm h^{-1} factor in their climatology of T11 < 235 K cloudiness. We prefer the rain rate units for the sake of easy discussion similar to *Mapes et al.* [2003a]. We also prefer this simple 3 mm h^{-1} factor to more complex calibrations because of the uncertainties involved.

[12] For the diurnal cycle analysis, we first calculate the June, July, and August 3-month average hourly (surface) or 3-hourly (satellite) precipitation at each grid or pixel. The resulting diurnal composite of precipitation is then

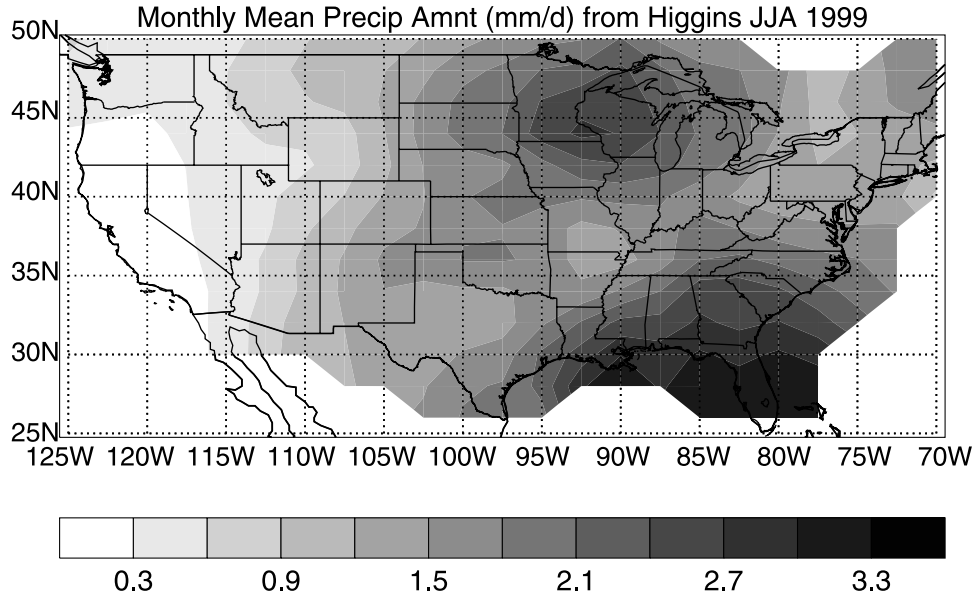

Figure 3. Summertime mean precipitation over the United States with resolution 2.5° longitude by 2.0° latitude based on surface data for 1999. See color version of this figure in the HTML.

decomposed spectrally using a Fourier transform to obtain the diurnal amplitude and phase following *Tian et al.* [2004].

3. Are Satellite IR Radiances Reliable for Inferring the Diurnal Cycle of Precipitation?

[13] Although the satellite radiances have been widely applied to study the diurnal cycle of tropical precipitation, the reliability of this approach has not been verified by independent surface observations. In this section, we compare the summertime precipitation and its diurnal cycle over the United States derived from the satellite radiances and surface observations to assess the reliability of this approach. Figures 4 and 5 show the diurnal amplitudes and phases over the United States with resolution 2.5° longitude by 2.0° latitude based on satellite radiances (Figure 4) and surface observations (Figure 5). The diurnal amplitude is denoted by the color shading and also by the

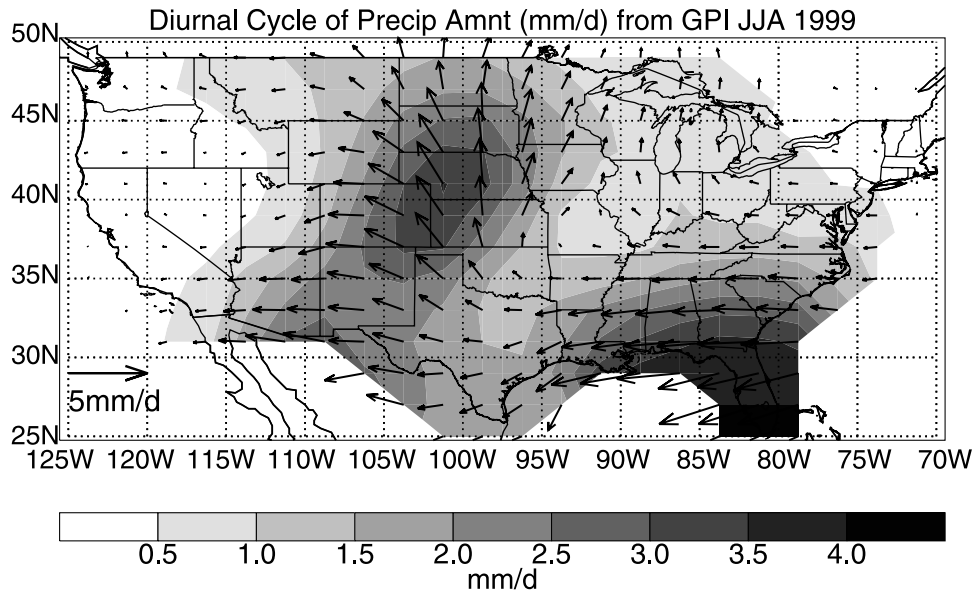

Figure 4. Diurnal cycle of summertime precipitation over the United States with resolution 2.5° longitude by 2.0° latitude based on satellite data for 1999. The diurnal amplitude is denoted by the shading and also by the length of the arrow (see inset key) (the same thereafter). The diurnal phase can be determined from the orientation of the arrows with respect to a 24-hour clock. Arrows pointing upward indicate a peak at 0000 LST (midnight), downward indicate a peak at 1200 LST (noon), toward the right indicate a peak at 0600 LST (dawn), and toward the left a peak at 1800 LST (sunset) (the same thereafter). See color version of this figure in the HTML.

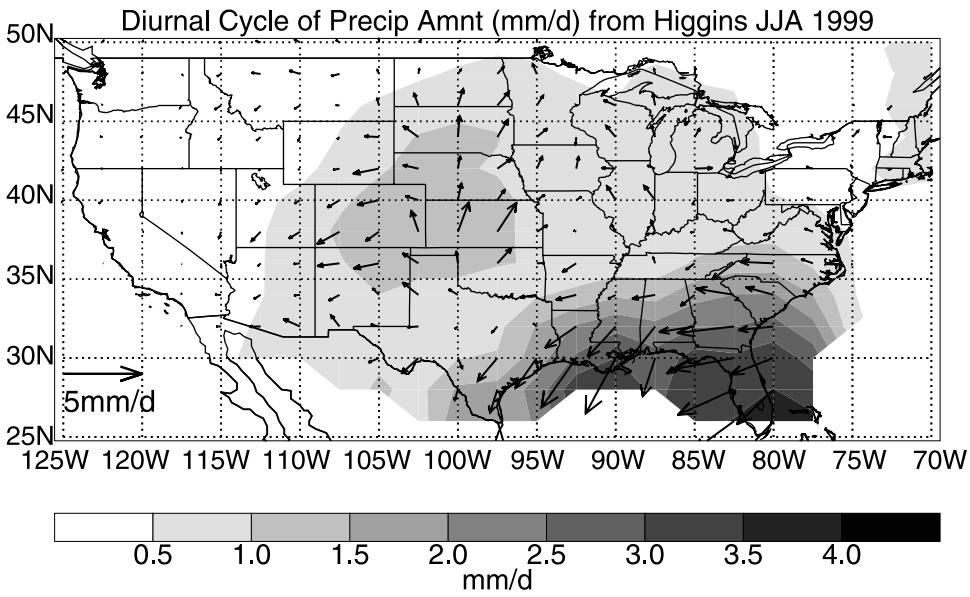

Figure 5. Diurnal cycle of summertime precipitation over the United States with resolution 2.5° longitude by 2.0° latitude based on surface data for 1999. See color version of this figure in the HTML.

length of the arrow (see inset key in Figures 4 and 5). The diurnal phase can be determined from the orientation of the arrows with respect to a 24-hour clock. Arrows pointing upward indicate a peak at 0000 local solar time (LST) (midnight), downward indicate a peak at 1200 LST (noon), toward the right indicate a peak at 0600 LST (dawn), and toward the left a peak at 1800 LST (sunset).

[14] Comparing the diurnal cycles between satellite retrievals (Figure 4) and surface observations (Figure 5) indicates that the diurnal pattern from the satellite retrievals is in broad agreement with surface observations. For example, both data sets show late afternoon maxima over the eastern, southeastern, and western United States including the Rocky Mountains and near midnight maxima over the Great Plains. Both data sets also agree on the regions of significant diurnal amplitude, such as the southeastern United States, especially Florida, and the Great Plains. The diurnal amplitudes are also comparable over most regions, except for the Great Plains, where the diurnal amplitudes from satellite retrievals are systematically larger than those from surface observations. This is due to the systematic biases of the GPI algorithm in the mean precipitation over the Great Plains (Figures 2 and 3). Over the Gulf coast, the diurnal phase from satellite data is a few hours later than from the surface data. This difference may be due to the different grid points in these two data sets (1.25° in longitude and 1.0° in latitude) or the course resolution of the data. Nonetheless, the broad agreement in the diurnal pattern from satellite retrievals and surface observations demonstrates that satellite radiances are reliable for inferring the diurnal cycle of precipitation, especially the diurnal phase.

4. Diurnal Cycle of Summertime Deep Convection and Precipitation Over NA

[15] The diurnal cycle of summertime convection and precipitation over NA at the spatial resolution 0.1° longitude by 0.1° latitude relying on the satellite radiances are presented in Figure 6. For clarity, the arrows are plotted every seven pixels with the arrows greater than 4 mm d^{-1} all having the same length, and the arrows less than 0.5 mm d^{-1} omitted. The prominent feature of the diurnal cycle over NA (Figure 6) is a land-sea contrast, consistent with the general characteristics of the diurnal cycle of tropical deep convection. Over the oceans, such as the Pacific Ocean, the Gulf of Mexico, and Atlantic Ocean, the diurnal cycle is weak with peaks near noon. Over most land regions, the deep convection tends to peak in the late afternoon and early evening with strong diurnal amplitudes, consistent with the thermodynamic response to the strong diurnal cycle of the land surface temperature. However, there are strong regional variations in both diurnal phases and amplitudes over land, suggesting that topography, land-sea contrast, and coastline curvature play an important role in modulating the diurnal cycle pattern. For example, near midnight maxima are found over the Great Plains, evidently associated with the eastern slope of the Rocky Mountains. The strong diurnal variation of the NAM rainfall, the largest diurnal amplitude over all of NA, is concentrated over the western slopes of the SMO. Furthermore, regional maxima in diurnal amplitudes are found over the Florida peninsula, the Yucatan peninsula, and the island of Cuba because of land-sea contrast and coastline curvature. Over the western United States, the diurnal amplitudes are generally small. In general, the regions of large diurnal amplitudes are also the regions of large daily mean precipitation, consistent with the general characteristics of the diurnal cycle of tropical deep convection [e.g., *Tian et al.*, 2004]. It is also interesting to note that the boundary between the late afternoon maxima over the western United States and the near midnight maxima over the Great Plains is the Continental Divide (106°W). Moreover, the boundary between the near midnight maxima over the Great Plains and the late afternoon maxima over the eastern and southeastern United States approximately follows the 200-m elevation line (Figures 1 and 6), running from southwest to northeast in the central

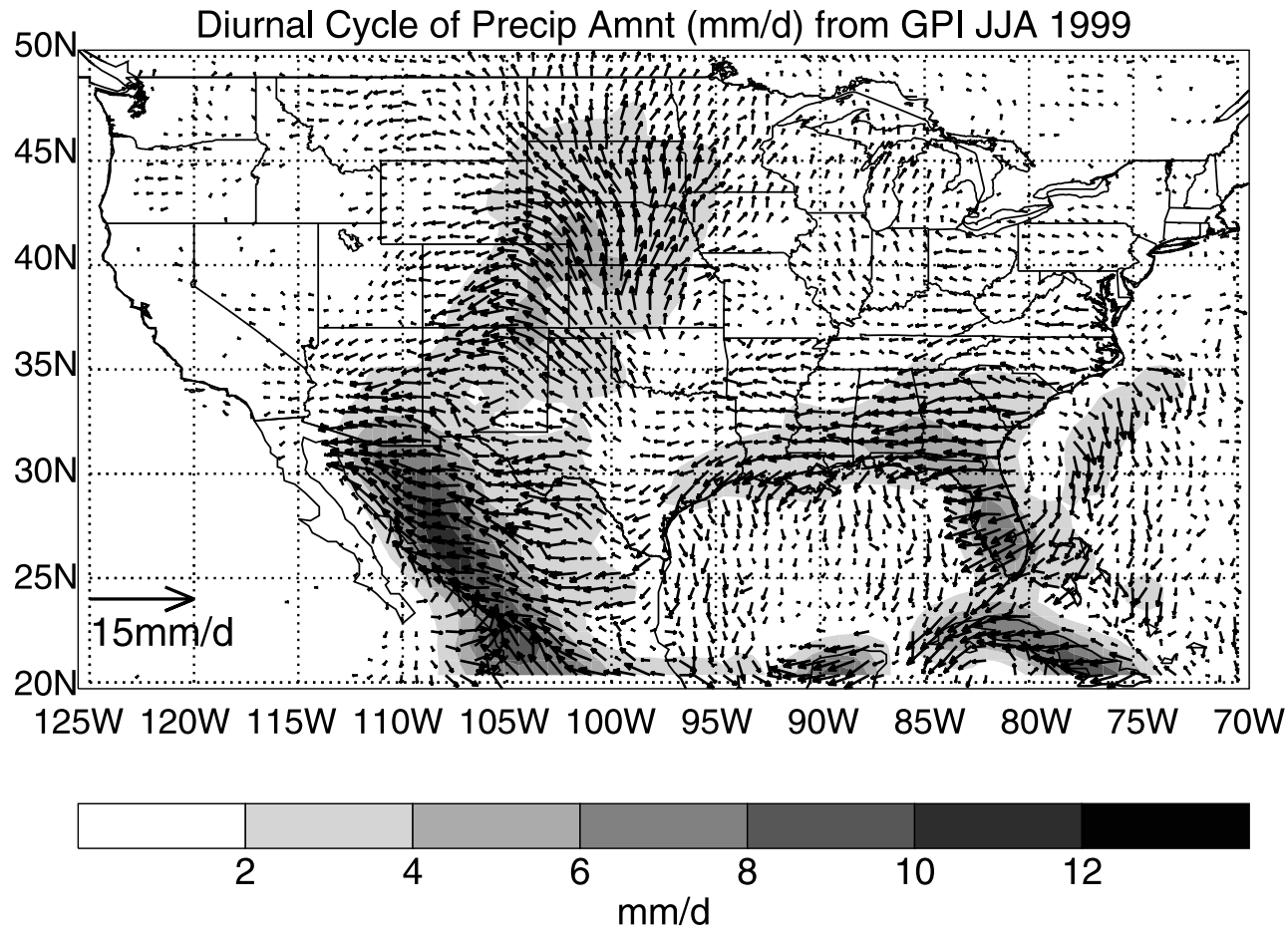

Figure 6. Diurnal cycle of summertime precipitation over NA at spatial resolution 0.1° longitude by 0.1° latitude based on satellite data for 1999. For clarity, the arrows are plotted every seven pixels with the arrows greater than 4 mm d^{-1} treated as 4 mm d^{-1} and the arrows lesser than 0.5 mm d^{-1} omitted. See color version of this figure at back of this issue.

United States. Along this boundary, the diurnal amplitudes are generally small.

[16] Over the coast of the Gulf of Mexico, the Florida peninsula, the Yucatan peninsula, and the island of Cuba, the convection and its diurnal cycle are strong with peaks in the late afternoon (1600–1800 LST). Over Florida, the maximum diurnal amplitude (around 9 mm d^{-1}) is found just southwest of the Lake Okeechobee over south Florida and the diurnal amplitude decreases from south to north and from inland peninsula to the coastal regions. Furthermore, the diurnal phase is earlier (around 1600 LST) over south Florida and shifts later to the north (around 1800 LST over Georgia and Alabama). Our results of the diurnal cycle over Florida are in broad agreement with previous observational studies based on surface station data, such as *Schwartz and Bosart* [1979]. We note that phase also shifts over the island of Cuba, from 1800 LST at the eastern tip to 1500 LST to the western tip. The phase then shifts back to 1800 LST as one moves over the Yucatan. The physical mechanisms responsible for the strong diurnal cycle over the coast of the Gulf of Mexico, the Florida peninsula, the Yucatan peninsula, and the island of Cuba are relatively well understood. It is generally accepted that the stronger diurnal cycle over most tropical/subtropical coastal areas, such as the coasts of the Gulf of Mexico, compared to most inland regions is the result of sea breeze fronts [e.g., *Atkinson*, 1981; *Pielke and Segal*, 1986; *Pielke*, 2001]. It is also generally accepted that the stronger diurnal cycle over most tropical/subtropical islands or peninsulas, such as Florida, Yucatan, and Cuba, compared to most coastal areas is due to the low-level convergence caused by sea breezes entering the islands or peninsulas from coasts [e.g., *Houze et al.*, 1981; *Yang and Slingo*, 2001]. This mechanism for the strong diurnal cycle over south Florida was initially pointed out by *Byers and Rodebush* [1948] and further validated by observational study by *Burpee* [1979] and three-dimensional numerical model simulation of the sea breezes by *Pielke* [1974].

[17] Over the Rocky Mountains, west of the Continental Divide (106°W), the convection and its diurnal cycle are weak with a peak at 1800 LST. In contrast, the diurnal cycle is strong with near a midnight maximum over the Great Plains, consistent with previous studies based on the surface station data, such as those of *Riley et al.* [1987] and *Dai et al.* [1999], and studies based on radar observations by *Carbone et al.* [2002]. Our high-resolution satellite data depict smooth transitions in the diurnal phase from late afternoon to early morning as the elevation decreases eastward from the Rocky Mountains to the Great Plains. The smooth diurnal phase shifts in our results demonstrate the spatial and temporal continuities of the diurnal cycle

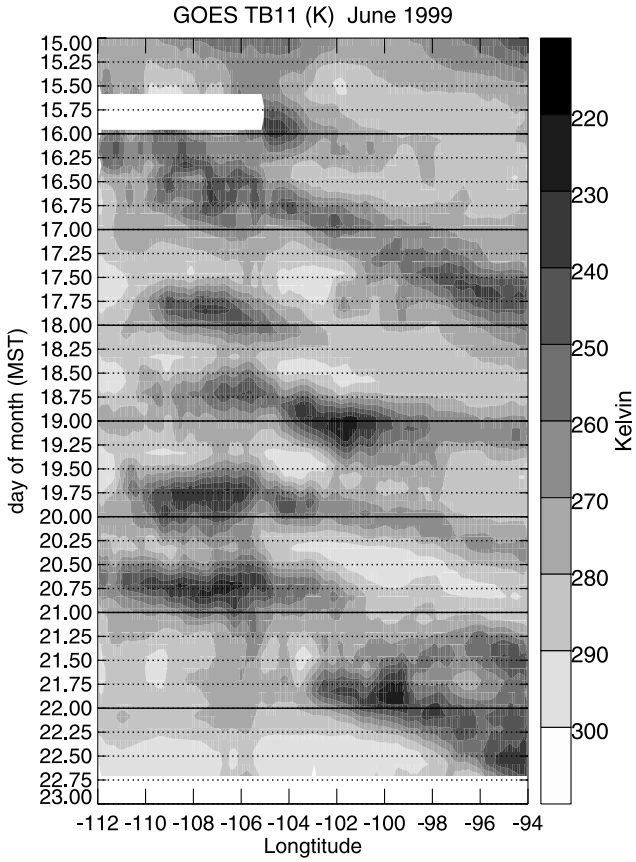

Figure 7. Hovmöller diagram of the satellite radiances over the Rocky Mountains and the Great Plains (averaged over 40°–41°N) for 10–23 June 1999. The Continental Divide is located around 106°W. The day of the month is in local time (mountain standard time (MST)). For example, x.00 indicates 0000 LT (midnight), x.25 indicates 0600 LT (dawn), x.50 indicates 1200 LT (noon), and x.75 indicates 1800 LT (sunset). See color version of this figure in the HTML.

over the Great Plains. They also support the mechanism proposed by *Riley et al.* [1987], who argued that the diurnal phase transitions of precipitation are highly suggestive of the convective precipitation systems forming in the mountains during the late afternoon and then spreading eastward onto the Great Plains. Recently, using radar observations, *Carbone et al.* [2002] documented the eastward propagation of precipitation systems. To further demonstrate this point, the Hovmöller (time-longitude) diagram of satellite radiances averaged over 40°–41°N for 15–23 June 1999 is shown in Figure 7. Eastward propagating convective systems are a prominent feature east of the Continental Divide, in stark contrast to the prevailing stationary convection over the mountains. The eastward propagating convective systems are generally initiated at or near the east slope of the Continental Divide (around 106°W) in the late afternoon and then propagate down the slope eastward and reach the Great Plains at night as in the *Carbone et al.* [2002] work. The propagation speed is about 15 m s^{-1}, often in excess of rates that are attributable either to the phase speeds of large-scale forcing or to advection from low-level to midlevel "steering" winds as pointed out by *Carbone et al.* [2002], who speculated that wavelike mechanisms, in the free troposphere and/or the planetary boundary layer, might contribute to the rates of motion observed [see also *Yang and Slingo*, 2001; *Mapes et al.*, 2003b]. *Toth and Johnson* [1985] also documented an eastward propagation of the upslope-to-downslope surface transition zones across the plains, which may also be responsible for this eastward propagation of convective systems.

[18] Afternoon convection is rare over the Great Plains. This is likely at least in part a result of daytime upslope wind blowing from the Great Plains to the Rockies, driven by the strong diurnal cycle of the mountain surface temperature and the sloping terrain of the Great Plains. Daytime upslope and nocturnal drainage flow [e.g., *Atkinson* 1981; *Pielke and Segal*, 1986; *Pielke*, 2001] is also a classic mesoscale atmospheric circulation, although less extensively studied compared to the land-sea breeze. *Toth and Johnson* [1985, Figure 10] found that the daytime flow over the Front Range of Colorado was dominated by a thermally induced easterly upslope flow. *Higgins et al.* [1997, Figure 10] also showed an afternoon easterly upslope wind over Texas based on reanalysis. The upward velocities associated with the upslope winds provide in the mountains an additional triggering mechanism for convection initiation in the afternoon. On the other hand, the downward return flow of the upslope wind suppresses the convection over the Great Plains in the afternoon, which may offset the diurnal forcing of the local surface temperature. In summary, the near midnight maxima of convection over the Great Plains result from the combination of a suppression of afternoon convection and the nighttime arrival of the eastward propagating convective systems, which are initiated at the Rocky Mountains in the previous afternoon.

[19] The mean precipitation and its diurnal cycle (plotted every three pixels) over the core NAM region are shown in Figures 8 and 9, respectively. The strong precipitation and diurnal cycle are concentrated over the western slopes of the SMO and run from northwest to southeast closely following the terrain lines with maxima at the elevation of around 1200 m. The precipitation and its diurnal cycle decrease rapidly both westward to the GC and eastward to the mountain peak and the east side of the SMO. On the west slopes of the SMO, the convection tends to peak around late afternoon and early evening (1800–2200 LST), while late afternoon (1800 LST) convection is dominant over the eastern side of the SMO. Over the GC, nocturnal convection is common but with weak amplitudes. However, over the mouth of the GC (~20°–24°N), the coastline is concave seaward and the spatial structures of convection and its diurnal cycle are different from the GC. First, strong convection is located not only onshore but also offshore (Figure 8). As a result, the maximum precipitation (12 mm d^{-1}) is located at the coast (105°W, 21.5°N) instead of farther inland. This is the most intense precipitation over the NAM region (Figure 8). Second, a significant diurnal cycle is found offshore in contrast to the small diurnal amplitudes over the GC. The diurnal amplitude decreases as one moves farther away from land. The land-sea contrast in diurnal phase is clear, with evening maximum onshore and morning maximum offshore; however, the transition at the coastline in not abrupt. Rather, the diurnal phase shifts very smoothly from evening at the coastal lands to early morning at the

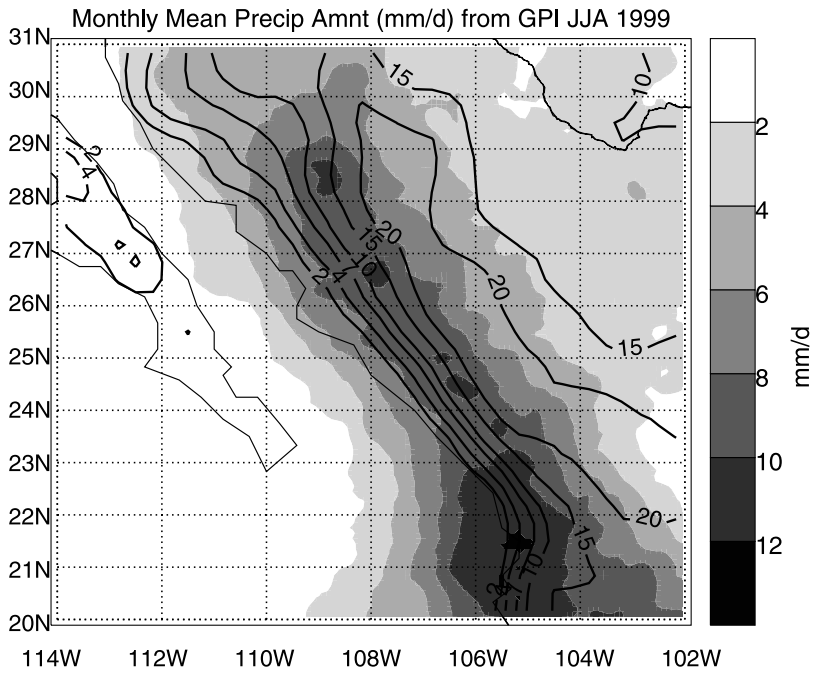

Figure 8. Summertime mean precipitation over the core NA monsoon (NAM) region. See color version of this figure at back of this issue.

coastal waters then to late morning farther offshore. The speed of the diurnal seaward sweep of convection is around 10 m s^{-1}. In general, our results are consistent with the studies by *Negri et al.* [1993, 1994] based on SSM/I but with important new information.

[20] The strong late afternoon and early evening convection over the western slopes of the SMO is easily understood and generally regarded as a result of the mountain lifting of a vigorous sea and valley breeze [e.g., *Negri et al.*, 1994; *Stensrud et al.*, 1995; *Berbery*, 2001]. The presence of mountains next to coast usually results in a circulation that blends the sea/land breeze and mountain/valley wind. Numerical simulations indicate that the combined circulation is much more intense than when they act separately

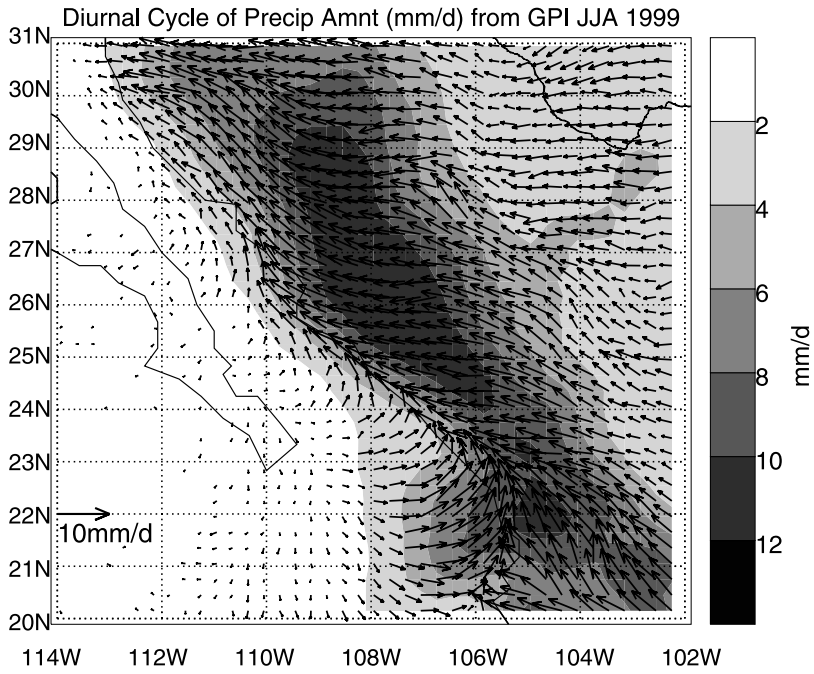

Figure 9. Diurnal cycle of summertime precipitation over the core NAM region. For clarity, the arrows are plotted every three pixels with the arrows greater than 6 mm d^{-1} treated as 6 mm d^{-1} and the arrows less than 0.5 mm d^{-1} omitted. See color version of this figure at back of this issue.

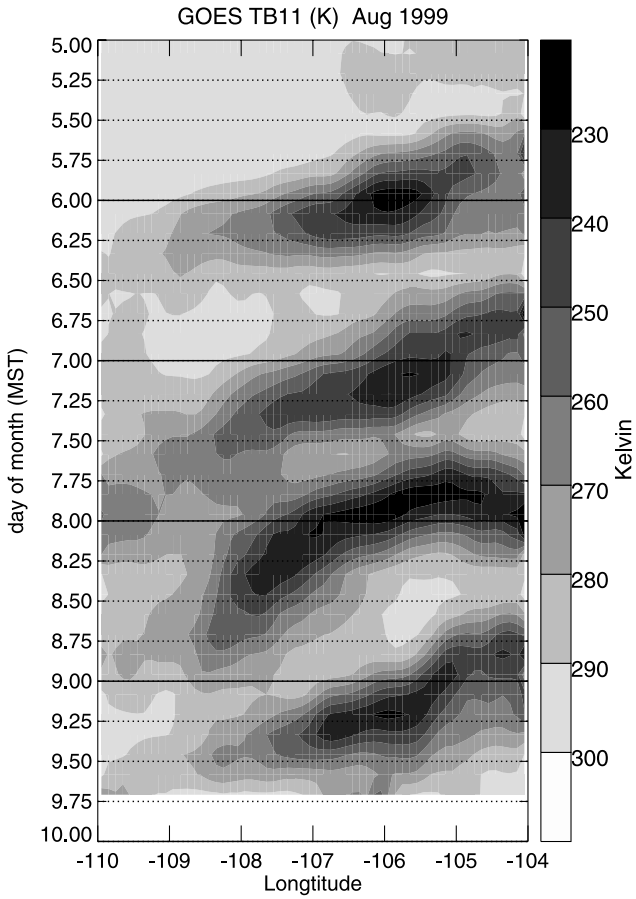

Figure 10. Hovmöller diagram of the satellite radiances over the mouth of the GC (averaged over 21.5°–22.5°N) for 5–10 August 1999. Please note that the coastline is located around 105.5°W. See color version of this figure in the HTML.

[e.g., *Mahrer and Pielke*, 1977]. This mountain lifting of the sea and valley breeze is an important initiation mechanism for afternoon convection over coastal mountains. However, the physical mechanisms responsible for the morning convection over the coastal waters are less clear. Traditionally, the offshore morning convection has been attributed to the offshore convergence of land/mountain breezes [e.g., *Houze et al.*, 1981; *Negri et al.*, 1994]. For example, if a land breeze meets a low-level prevailing flow offshore [e.g., *Ramage*, 1965; *Kousky*, 1980; *Houze et al.*, 1981] or the coastline is concave seaward [e.g., *Negri et al.*, 1994; *Ohsawa et al.*, 2001; *Zuidema*, 2003], the land breezes will tend to convergence offshore, which will initiate deep convection over the coastal waters. Since the Mexican coastline is concave seaward over the mouth of the GC, the offshore convergence of the nocturnal drainage flows and land breezes from the SMO to the GC may be responsible for the offshore morning convection found here. However, *Mapes et al.* [2003b] has argued that nighttime radiative cooling of land and the associated thermal land breezes are much weaker than the corresponding daytime sea breezes, especially under humid tropical skies. Most importantly, the convergence of land breezes cannot explain the gradual diurnal phase shift in the satellite data (Figure 9). Thus the land breeze convergence may not be the complete explanation of nocturnal convection in coastal areas.

[21] Similar to the Great Plains, the smooth diurnal phase shifts over the mouth of the GC demonstrate the spatial and temporal continuities of the diurnal cycle over this region. They also indicate that the morning convection over the waters may be developed over the coastal mountains in the previous evening. To demonstrate this point, the Hovmöller (time-longitude) diagram of satellite radiances averaged over 21.5°–22.5°N for 5–10 August 1999 is shown in Figure 10. Westward (seaward) propagating convective systems are the dominant features over this region. The convective systems are generally initiated in the evening at the coastal mountains, in response to the diurnal heating of mountain surface temperature and then propagate westward over the oceans after midnight and gradually dissipate. These westward propagating systems can explain the morning convection, the smooth diurnal phase and diurnal amplitude decrease over the waters (Figures 8 and 9). The seaward propagating convective systems may be a result of a seaward propagating diurnal gravity wave in the planetary boundary layer radiating from the coastal mountain mixed layer as proposed by *Yang and Slingo* [2001] and *Mapes et al.* [2003b].

5. Summary

[22] The principal findings of this study are the following:

[23] 1. Comparing the diurnal cycle over the United States between satellite retrievals and surface observations indicates that the diurnal pattern from the satellite retrievals is in broad agreement with surface observations. This demonstrates that satellite radiances are reliable for inferring the diurnal cycle of precipitation, especially the diurnal phase.

[24] 2. Over most land regions, deep convection peaks in the late afternoon and early evening, a few hours later than the peak of land surface temperature, indicating that the diurnal cycle of continental convection can be mainly attributed to a direct thermodynamic response to the strong diurnal cycle of land surface temperature. However, strong regional variations exist in both diurnal phase and amplitude over NA, implying that topography, land-sea contrast, and coastline curvature play an important role in modulating the diurnal cycle.

[25] 3. Over the coast of the Gulf of Mexico, the Florida peninsula, the Yucatan peninsula, and the island of Cuba, the precipitation and its diurnal cycle are strong with peaks in the late afternoon (1600–1800 LST). Over Florida, the maximum diurnal amplitude (around 9 mm d^{-1}) is found just southwest of the Lake Okeechobee over south Florida and the diurnal amplitude decreases from south to north and from inland peninsula to the coastal regions. Furthermore, the diurnal phase is earlier (around 1600 LST) over south Florida and shifts later to the north (around 1800 LST over Georgia and Alabama). The strong diurnal cycle over the coast of the Gulf of Mexico, the Florida and Yucatan peninsulas, and the island of Cuba is the result of sea breeze fronts and/or the low-level convergence caused by sea breezes entering the islands or peninsulas from coasts.

[26] 4. Near midnight maxima of precipitation are found over the Great Plains with smooth transitions in the diurnal phase from late afternoon to early morning over the Great

Plains. Satellite data also demonstrate that the near midnight convection over the Great Plains is the result of the combination of a suppression of afternoon convection and the nighttime arrival of the eastward propagating convective systems initiated at the Rocky Mountains in the previous afternoon.

[27] 5. Over northwestern Mexico, strong precipitation and diurnal cycle are concentrated over the western slopes of the SMO and run from northwest to southeast closely following the terrain lines with maxima at the elevation of around 1200 meters. The diurnal cycle decreases rapidly both westward to the GC and eastward to the mountain peak. On the west slopes of the SMO, the convection peaks around late afternoon and early evening (1800–2200 LST), while late afternoon (1800 LST) convection is dominant over the eastern side of the SMO. The strong late afternoon and early evening convection over the western slopes of the SMO is a result of the mountain lifting of a vigorous sea and valley breeze. Over the GC, nocturnal convection is common but with weak amplitudes. However, over the mouth of the GC, significant diurnal cycles are found offshore with amplitude decreasing from coastal waters farther offshore. Furthermore, the diurnal phase shifts smoothly from early morning at the coastal waters to late morning farther offshore. Satellite data demonstrate that the morning convection offshore is the result of the westward propagating convective systems initiated at the coastal mountains in the previous evening.

[28] 6. This study emphasizes the need for better representation of the effects of mountain-valley winds, land-sea breezes, and diurnally forced gravity waves over regions of complex topography, land-sea contrast, and coastline curvature in order to improve the diurnal cycle simulation in climate models.

[29] **Acknowledgments.** We wish to thank Xiangqian Wu for providing us with the satellite data and Siegfried D. Schubert, Myong-In Lee, and Hyun-Kyung Kim for providing the surface precipitation data and for their assistance in analyzing the data, as well as Keith Dixon for providing the 20-min surface relief data. Discussions with Jeff Ploshay and the comments from GFDL internal reviewers Eric M. Wilcox and Stephen T. Garner as well as two anonymous external reviewers are appreciated. This research was supported in part by ARM grant DE-AI02-00ER62900.

References

Arkin, P. A., and B. N. Meisner (1987), The relationship between large-scale convective rainfall and cold cloud over the western hemisphere during 1982–84, *Mon. Weather Rev.*, *115*, 51–74.

Atkinson, B. W. (1981), *Meso-scale Atmospheric Circulations*, 495 pp., Elsevier, New York.

Berbery, E. H. (2001), Mesoscale moisture analysis of the North American monsoon, *J. Clim.*, *14*, 121–137.

Burpee, R. W. (1979), Peninsula-scale convergence in the south Florida sea breeze, *Mon. Weather Rev.*, *107*, 852–860.

Byers, H. R., and H. R. Rodebush (1948), Causes of thunderstorms of the Florida peninsula, *J. Meteorol.*, *6*, 275–280.

Carbone, R. E., J. D. Tuttle, D. A. Ahijevych, and S. B. Trier (2002), Inferences of predictability associated with warm season precipitation episodes, *J. Atmos. Sci.*, *59*, 2033–2056.

Dai, A., F. Giorgi, and K. E. Trenberth (1999), Observed and model-simulated diurnal cycles of precipitation over the contiguous United States, *J. Geophys. Res.*, *104*, 6377–6402.

Garreaud, R. D., and J. M. Wallace (1997), The diurnal march of convective cloudiness over the Americas, *Mon. Weather Rev.*, *125*, 3157–3171.

Gray, W. M., and R. W. Jacobson (1977), Diurnal variation of deep cumulus convection, *Mon. Weather Rev.*, *105*, 1171–1188.

Higgins, R. W., J. E. Janowiak, and Y. Yao (1996), A gridded hourly precipitation data base for the United States (1963–1993), in *NCEP/Climate Prediction Center Atlas*, vol. 1, 47 pp., Natl. Weather Serv., Camp Springs, Md.

Higgins, R. W., Y. Yao, E. S. Yarosh, J. E. Janowiak, and K. C. Mo (1997), Influence of the Great Plains low-level jet on summertime precipitation and moisture transport over the central United States, *J. Clim.*, *10*, 481–507.

Houze, R. A., Jr., S. G. Geotis, F. D. Marks Jr., and A. K. West (1981), Winter monsoon convection in the vicinity of north Borneo. part I: Structure and time variation of the clouds and precipitation, *Mon. Weather Rev.*, *109*, 1595–1614.

Joyce, R., and P. A. Arkin (1997), Improved estimates of tropical and subtropical precipitation using the GOES precipitation index, *J. Atmos. Oceanic Technol.*, *14*, 997–1011.

Kousky, V. E. (1980), Diurnal rainfall variation in northeast Brazil, *Mon. Weather Rev.*, *108*, 488–498.

Landin, M. G., and L. F. Bosart (1989), The diurnal variation of precipitation in California and Nevada, *Mon. Weather Rev.*, *117*, 1801–1816.

Mahrer, Y., and R. A. Pielke (1977), The effects of topography on sea and land breezes in a two-dimensional numerical model, *Mon. Weather Rev.*, *105*, 1151–1162.

Mapes, B. E., T. T. Warner, M. Xu, and A. J. Negri (2003a), Diurnal patterns of rainfall in northwestern South America. Part I: Observations and context, *Mon. Weather Rev.*, *131*, 799–812.

Mapes, B. E., T. T. Warner, and M. Xu (2003b), Diurnal patterns of rainfall in northwestern South America. Part III: Diurnal gravity waves and nocturnal convection offshore, *Mon. Weather Rev.*, *131*, 830–844.

Meisner, B. N., and P. A. Arkin (1987), Spatial and annual variations in the diurnal cycle of large-scale tropical convective cloudiness and precipitation, *Mon. Weather Rev.*, *115*, 2009–2032.

Neale, R., and J. Slingo (2003), The maritime continent and its role in the global climate: A GCM study, *J. Clim.*, *16*, 834–848.

Negri, A. J., R. Adler, R. A. Maddox, K. W. Howard, and P. R. Keehn (1993), A regional rainfall climatology over Mexico and the southwest United States derived from passive microwave and geosynchronous infrared data, *J. Clim.*, *6*, 2144–2161.

Negri, A. J., R. F. Adler, E. J. Nelkin, and G. J. Huffman (1994), Regional rainfall climatologies derived from Special Sensor Microwave Imager (SSM/I) data, *Bull. Am. Meteorol. Soc.*, *75*, 1165–1182.

Ohsawa, T., H. Ueda, T. Hayashi, A. Watanabe, and J. Masumoto (2001), Diurnal variations of convective activity and rainfall in tropical Asia, *J. Meteorol. Soc. Jpn.*, *79*, 333–352.

Pielke, R. A. (1974), A three-dimensional numerical model of the sea breezes over south Florida, *Mon. Weather Rev.*, *102*, 115–139.

Pielke, R. A. (2001), *Mesoscale Meteorological Modeling*, *Int. Geophys. Ser.*, vol. 78, 2nd ed., 676 pp., Elsevier, New York.

Pielke, R. A., and M. Segal (1986), Mesoscale circulations forced by differential terrain heating, in *Mesoscale Meteorology and Forecasting*, edited by P. S. Ray, pp. 516–548, Am. Meteorol. Soc., Boston, Mass.

Ramage, C. S. (1965), Diurnal variation of summer rainfall over Malaya, *J. Trop. Geogr.*, *19*, 62–68.

Riley, G. T., M. G. Landin, and L. F. Bosart (1987), The diurnal variability of precipitation across the central Rockies and adjacent Great Plains, *Mon. Weather Rev.*, *115*, 1161–1172.

Schwartz, B. E., and L. F. Bosart (1979), The diurnal variability of Florida rainfall, *Mon. Weather Rev.*, *107*, 1535–1545.

Stensrud, D. J., R. L. Gall, S. L. Mullen, and K. W. Howard (1995), Model climatology of the Mexican monsoon, *J. Clim.*, *8*, 1775–1794.

Tian, B., B. J. Soden, and X. Wu (2004), Diurnal cycle of convection, clouds, and water vapor in the tropical upper troposphere: Satellites versus a general circulation model, *J. Geophys. Res.*, *109*, D10101, doi:10.1029/2003JD004117.

Toth, J. J., and R. H. Johnson (1985), Summer surface flow characteristics over northeast Colorado, *Mon. Weather Rev.*, *113*, 1458–1469.

Trenberth, K. E., A. Dai, R. M. Rasmussen, and D. B. Parsons (2003), The changing character of precipitation, *Bull. Am. Meteorol. Soc.*, *84*, 1205–1217.

U.S. CLIVAR Pan American Implementation Panel (2002), U.S. CLIVAR Pan American research: A scientific prospectus and implementation plan, report, 58 pp., U.S. CLIVAR Off., Washington, D. C.

Wallace, J. M. (1975), Diurnal variations in precipitation and thunderstorm frequency over the conterminous United States, *Mon. Weather Rev.*, *103*, 406–419.

Yang, G.-Y., and J. M. Slingo (2001), The diurnal cycle in the tropics, *Mon. Weather Rev.*, *129*, 784–801.

Zuidema, P. (2003), Convective clouds over the Bay of Bengal, *Mon. Weather Rev.*, *131*, 780–798.

I. M. Held, N.-C. Lau, and B. J. Soden, Geophysical Fluid Dynamics Laboratory, NOAA, Princeton, NJ 08542, USA.

B. Tian, California Institute of Technology, MS 150-21, 1200 East California Blvd., Pasadena, CA 91125, USA. (btian@gps.caltech.edu)

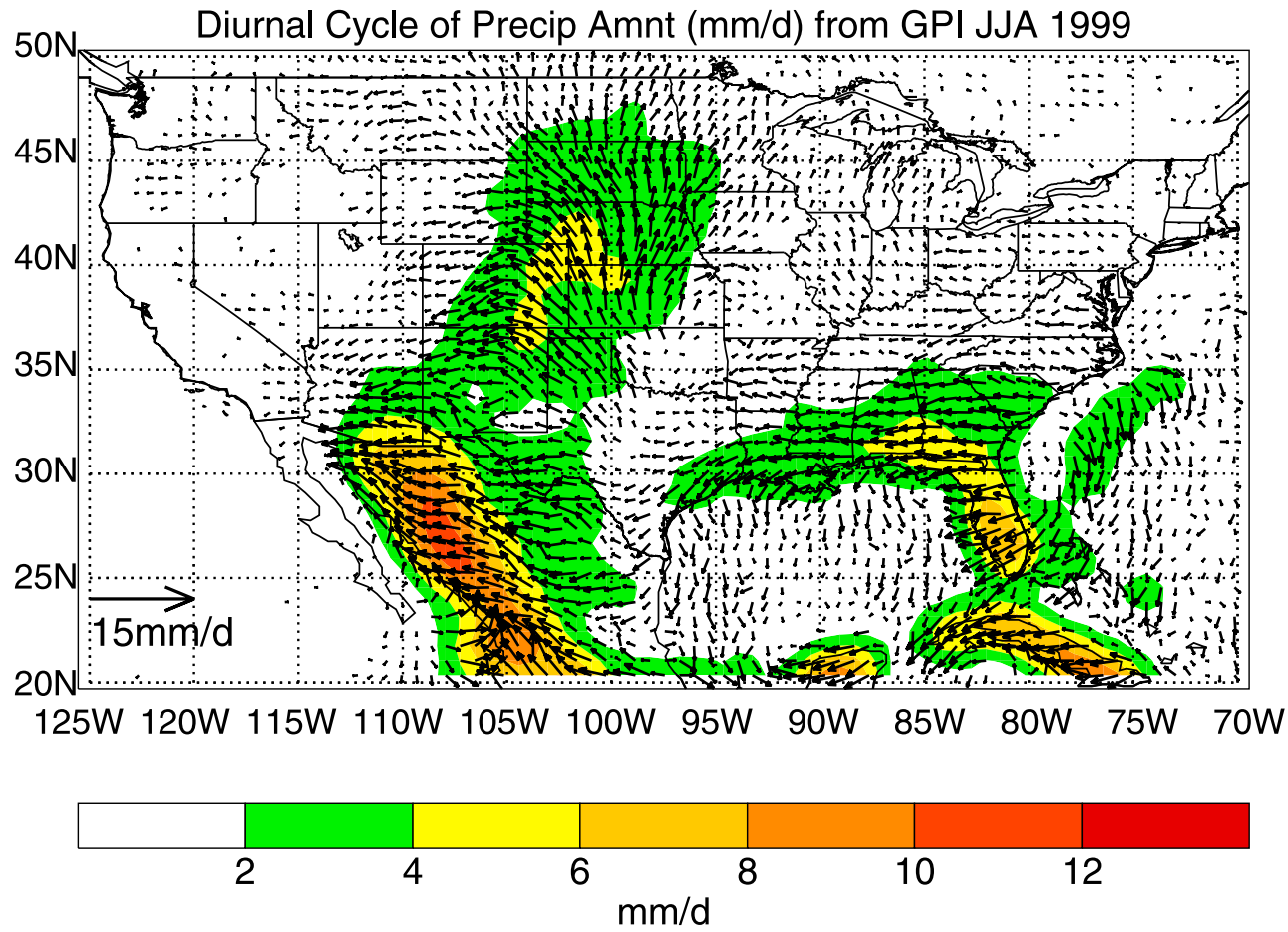

Figure 6. Diurnal cycle of summertime precipitation over NA at spatial resolution 0.1° longitude by 0.1° latitude based on satellite data for 1999. For clarity, the arrows are plotted every seven pixels with the arrows greater than 4 mm d^{-1} treated as 4 mm d^{-1} and the arrows lesser than 0.5 mm d^{-1} omitted.

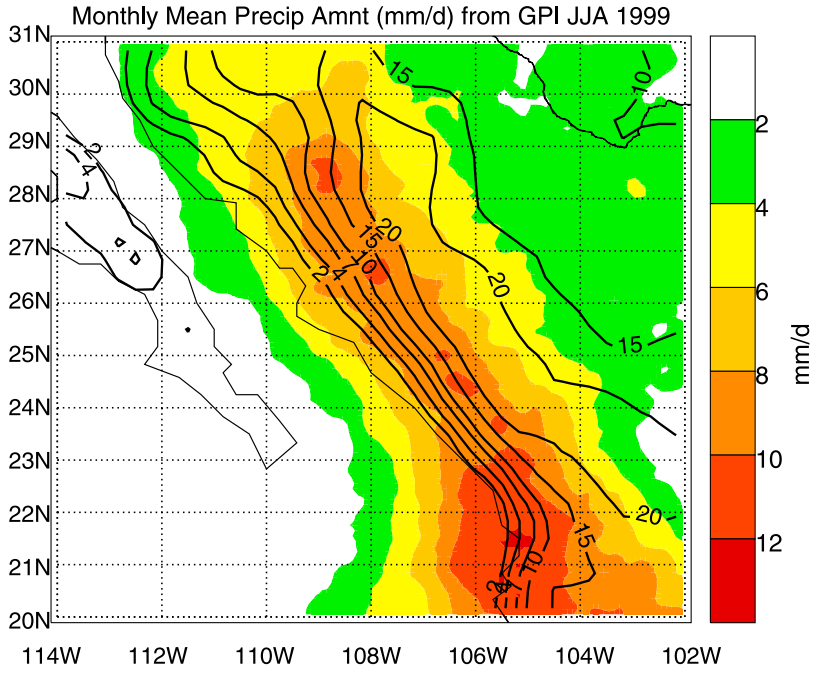

Figure 8. Summertime mean precipitation over the core NA monsoon (NAM) region.

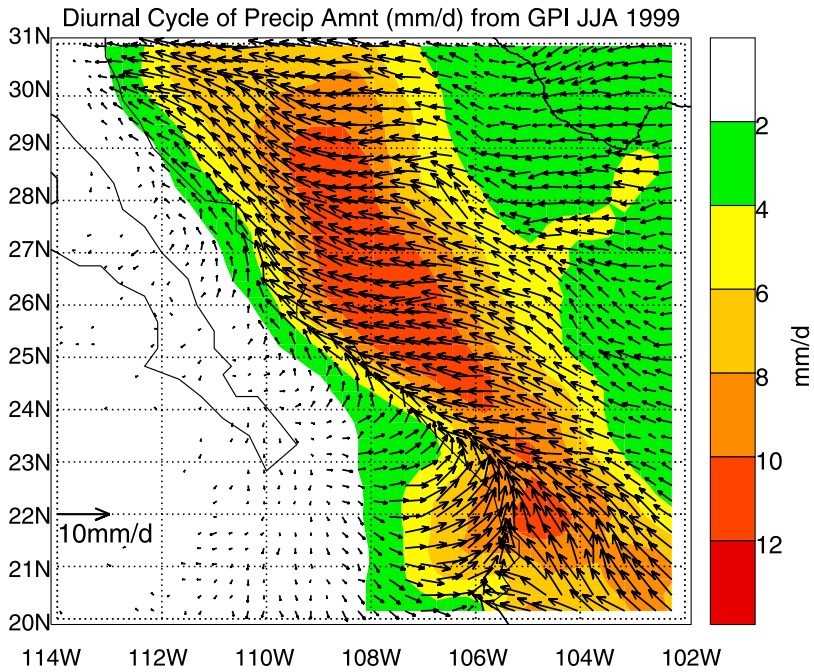

Figure 9. Diurnal cycle of summertime precipitation over the core NAM region. For clarity, the arrows are plotted every three pixels with the arrows greater than 6 mm d^{-1} treated as 6 mm d^{-1} and the arrows less than 0.5 mm d^{-1} omitted.